



Study the Effect of Welding Heat Input on the Microstructure, Hardness, and Impact Toughness of AISI 1015 Steel

Emad Kh. Hamd* Abbas Sh. Alwan** Ihsan Khalaf Irthiea***

*,*** Engineering college/University of Anbar/ Iraq

** Agriculture College/University of Baghdad/Iraq

*Email: emkh7676@gmail.com

**Email: drabbasshalwan@gmail.com

***Email: ih77san@yahoo.co.uk

(Received 17 May 2017; accepted 31 august 2017)

<https://doi.org/10.22153/kej.2018.08.005>

Abstract

In the present study, MIG welding is carried out on low carbon steel type (AISI 1015) by using electrode ER308L of 1.5mm diameter with direct current straight polarity (DCSP). The joint geometry is of a single V-butt joint with one pass welding stroke for different plate thicknesses of 6, 8, and 10 mm. In welding experiments, AISI 1015 plates with dimensions of 200×100mm and edge angle of 60° from both sides are utilized. In this work, three main parameters related to MIG welding process are investigated, which are welding current, welding speed, heat input and plate thickness, and to achieve that three groups of plates are employed each one consists of three plates. The results indicate that increasing the weld heat input (through changing the current and voltage) leads to an increase in widmanstatten ferrite (WF), acicular ferrite (AF) and polygonal ferrite (PF) in FZ region, and a reduction in grain size. It is observed that the micro-hardness of welded AISI 1015 plate increases as the weld heat input decreases. As well as increasing the weld heat input results in an increase in the width of WM and HAZ and a reduction in the impact energy of the weld joint of AISI 1015 at WM region. Also, it is noted the corrosion rate of weld joint increases with increase of Icorr due to increasing in welding current (heat input), corrosion rate increased up to (0.126µm/yr.) with increasing of heat input up to (1.27 KJ/mm).

Keywords: Heat input, impact trength, MIG welding, micro-hardness.

1. Introduction

Numerous welding systems are utilized to create fabricated assemblies that may not seem to incorporate welding by any means. Welding additionally has key applications for the repair of basic structural assemblies. Welding procedures are advantageously separated into two classes: fusion welding and solid state welding [1].

The high temperature associated to fusion welding may cause entrapping some oxides in the weld metal and this action in turn degrade the mechanical properties and corrosion resistance of the weld joint. In all electric arc welding processes, a gaseous shield is therefore created

around the weld zone to protect it from surrounding atmosphere [2-3].

It is found that the process key parameters of metal inert gas (MIG) have a crucial influence on the quality, productivity and cost of welding joints [4-6]. MIG welding process overcome the constraint of using small lengths of electrodes as in manual metal arc welding and overcomes the incapability of the submerged arc process to weld in a number of positions. It is not surprising, therefore, that the 50/50 level of the relative weights of weld metal deposited by manual metal arc and MIG processes was reached in 1973 in the USA and in 1978 in Europe [7].

Reverse polarity (positive electrode) is used for most MIG welds. This arrangement offers more stable arc than the straight polarity arrangement, and faster welding speeds are possible. The latter results from electrons striking the consumable electrode (welding wire) which is more rapidly melted and deposited into the joint area. Moreover, as MIG welding includes the transfer of metal droplets from the electrode to the base metal, relatively deeper penetration is acquired with reverse polarity. If straight polarity is used, the large positive ions travelling toward the electrode tend to support the metal droplets, which results in shallow weld penetration. Conversely, the metal droplets are subjected to a significant downward force by the large positive ions when reverse polarity is used, which results in greater depth penetration [1]. This work presents an experimental investigation on the

effect of some MIG process parameters such as weld heat input, weld current and weld speed on the microstructure (grain size), microhardness, and impact resistance of MIG weldment.

2. Experimental Work

2.1. Materials

In the current work plates of low carbon steel (AISI-1015) are used as base metal for the welding processes. The experimental chemical composition of the material and the standard composition of AISI-or SAE 1015 according to (SWE) are shown in Table 1. The standard mechanical properties of the AISI 1015 carbon steel are displayed in Table 2.

Table 1,
The chemical composition of low carbon steel

Element	C%	Si%	Mn%	P%	S%	Cr%
Measured Wt.%	0.148	0.065	0.537	0.016	0.004	0.0033
	Mo%	Ni%	Al%	Cu%	Fe%	
	<0.002	0.055	0.054	0.071	Bal.	
Standard AISI 1015 [8]	C%	Mn%	P. max%	S. max%	Fe%	
	0.13-018	0.3-0.6	0.04	0.05	Bal.	

Table 2,
The standard mechanical properties of the AISI-1015 [8]

Properties	Condition	
	HF	CF
Tensile strength (MPa)	324	365
Yield strength (MPa)	179	303
Elongation (in 2 in. %)	28	20

2.2. Experiment Procedure

The plates of low carbon steel with dimensions of (200 mm Long \times 100 mm Width, with different thicknesses were prepared by milling machine from both surfaces and V- single butt joint is designed by machining the specimen to angle (60°) from both sides as shown in Fig. 1. Nine samples of weldments at different parameters were prepared as shown in Table 3. Plate thickness of specimens 7, 8 and 9 with thickness 6, 8 and 10mm respectively. Metal Inert Gas welding (MIG) process is executed using consumable electrode ER308L austenitic stainless steel of diameter (1.5mm) conforms to certification: AWS A5.9/ASME SFA A5.9, it contains low carbon content and this help to prevent the intergranular corrosion. MIG welding

machine used in this work was type (ESAB), Ideal arc DC-600-Lincoln Company- Sweden. MIG welding is carried out with one pass, and an electrode ER308L of diameter (1.5mm). A stop watch was used to record the welding time. All samples for microstructure prepared after cutting and SiC emery paper of grade 120, 320, 500, 1000, and 1200. Slurry of Al₂O₃ particles of size of 5 μ m were used for polishing Process, with a special cloth. Etching process was carried out using Nital solution consisting of 2% nitric acid (HNO₃) and 98% of alcohol. The optical microscopy type RGH, with digital camera connected to the computer at magnification \times 200 is used for microstructure examination. J-image software and linear intercept method are used to measure the average grain size. The heat input (KJ/mm) is calculated by equation:

$$(Q=\eta \times (VI/v) (\eta=0.7) \quad \dots(1)$$

Microhardness test by using digital microhardness tester type (QV-100-Qualitest company-Japan). Microhardness traverses 1mm (the distance between two readings), were produced across the weld regions using a 1000g load and a 10sec dwell time. To conduct the Impact test, firstly test piece is prepared based on standard ASTM A370, (the standard specimen size for Charpy impact testing is (10mm×10 mm×55 mm). The energy toughness values are recorded to evaluate the effect of heat input on the impact strength of weldments as shown in Table 4.

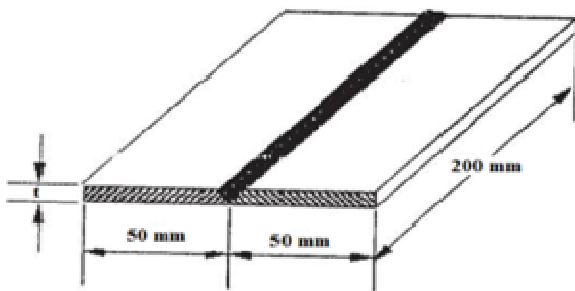


Fig. 1. Single V-joint design of plate.

Table 4,
Welding parameters of weldments for Impact test.

Specimen Code.	Plate Thickness (mm)	Welding Current (Amp)	Welding Voltage (volt)	Welding Speed (mm/min)	Heat Input (KJ/mm)
A	10	220	20.7	150.37	1.2719
B	10	240	21.7	150.37	1.4546
C	10	260	23	150.37	1.6702

3. Results

3.1. Effect of Weld Speed on Microstructure

Increasing welding speed results in decreasing heat input as shown in Fig. 2. The effect of heat input is to decrease grain size of weld metal (WM) and heat affected zone (HAZ), but no effect on grain size of base metal. Increasing of welding speed (decreasing of heat input) cause a little decrease of ferrite grain size about 11% as a decreasing percentage as shown in Table 5, due to increasing the cooling rate. The microstructure of weld metal (FZ) is consisting mainly of acicular ferrite (AF), Widmanstatten ferrite (WF) and

Table 3,
Experimental welding conditions of MIG welding.

Specimen	Variables	
1		172.413
2	Speed Welding (v) (mm/min)	150.37
3		100
4		180
5	Current Welding (I) (Ampere)	190
6		210
7	Plate Thickness (t) (mm)	6
8		8
9		10

polygonal ferrite (PF), and refine with increase the welding speed (decrease heat input) as shown in Figs. 3, 4 and 5. Also, the microstructure of HAZ grains are also refined with decreasing heat input. From Table 5, the grain boundary is also affected by cooling rates (heat input) which depend on welding parameters such as welding current and speed. When increase the welding speed leads to a slight decrease in grain size in FZ and HAZ, but the grain size of BM has not affected. Grain refinement is resulted at lower heat input (faster cooling rate). This is in agreement with the reference [9].

Table 5,
Calculation result of heat input and grain size with different welding conditions.

Specimen	Heat Input (KJ/mm)	Grain Size (µm)			Width (mm)	
		FZ	HAZ	BM	FZ	HAZ
1	0.826	16.85	17		4	4
2	0.945	17	17.82		4.5	3.5
3	1.428	18.94	18.85		5	3.5
4	0.763	11.77	12		4	3.5
5	0.805	14.27	13.47	20.19	4.5	4
6	0.889	20.6	17.24		5	5
7	1.2719	10.68	11.2		3	2
8	1.6408	12.44	12.7		3.5	3
9	2.5116	14.77	12.3		4	3.5

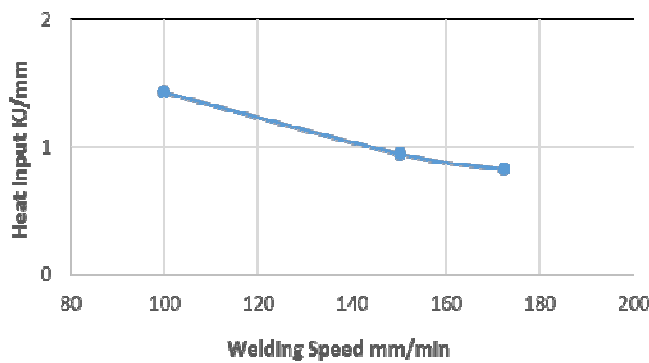


Fig. 2. The relationship between Heat Input and Welding Speed at 170 Amp and 20 volt.

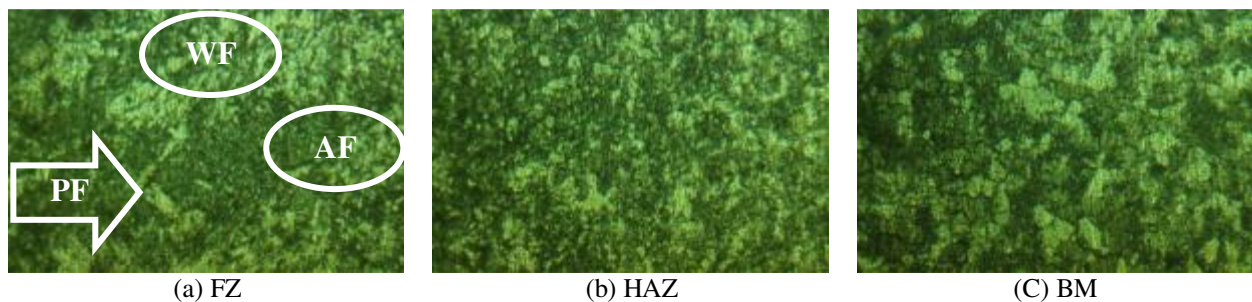


Fig. 3. Microstructure of butt joint of specimen 1 at I: 170Amp, V: 20volt, S: 172.413mm/min and Heat Input: 0.826 KJ/mm, (×200).



Fig. 4. Microstructure of butt joint of specimen 2 at I: 170Amp, V: 20volt, S: 150.37mm/min and Heat Input: 0.945 KJ/mm, (×200).



Fig. 5. Microstructure of butt joint of specimen 3 at I: 170Amp, V: 20volt, S: 100mm/min and Heat Input: 1.428 KJ/mm, (×200).

3.2. Effect of Weld Current on Microstructure

It is observed that the heat input increases with the welding current as shown in Fig. 6. A columnar grain was course as seen in the weld metal (fusion zone). Therefore, an increase in the welding current leads to increase grain size as shown in Table 5. An increase in welding current effect on increase of the grain size in both FZ and HAZ regions. This variation in grain size due to

the effect of cooling rates. The microstructure of fusion zone consists of fine acicular ferrite (AF), Widmanstatten ferrite (WF) and some inclusions as shown in Figs. 7 and 8. The size of HAZ region grains increases with increasing welding current (increase heat input) as illustrated in Table 5. The increase in welding current causes the heat generated to increase resulting the polygonal ferrite grains in FZ to recrystallized and grow as presented in Fig. 9.

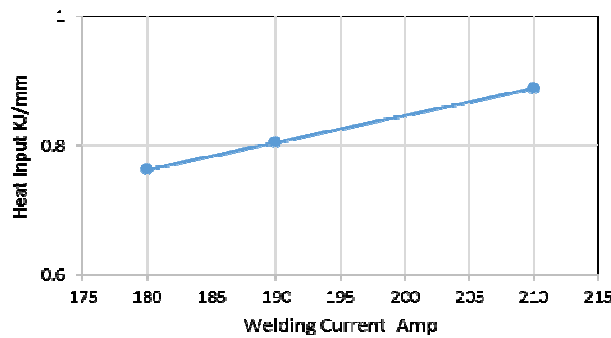


Fig. 6. The relationship between Heat Input and Welding Current at welding Speed 200mm/min, and welding voltage 20.2volt.

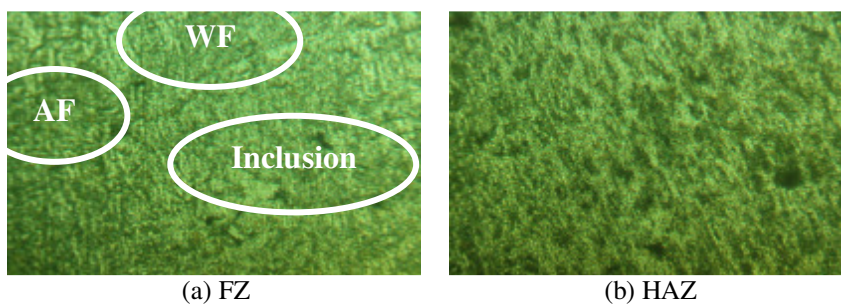


Fig. 7. Microstructure of butt joint of specimen 4 at I: 180Amp, V: 20.2volt, S: 200mm/min and heat input 0.763 KJ/mm, (×200).

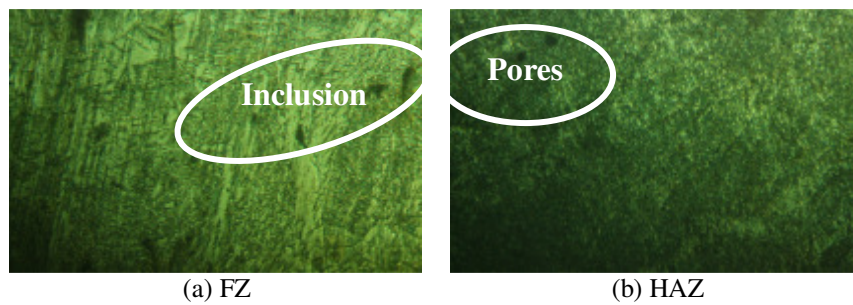


Fig. 8. Microstructure of butt joint of specimen 5 at I: 190Amp, V: 20.2volt, S: 200mm/min and heat input 0.805 KJ/mm, ($\times 200$).

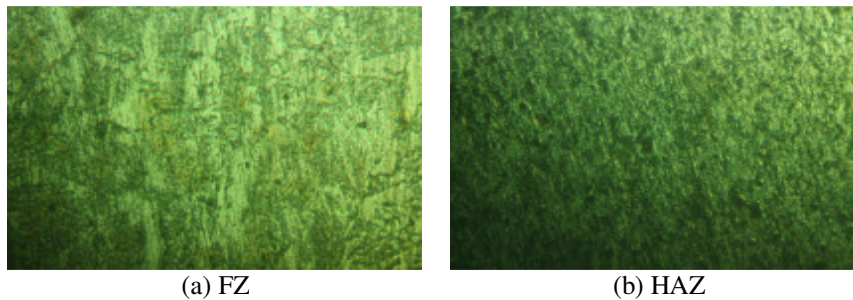


Fig. 9. Microstructure of butt joint of specimen 6 at I: 210Amp, V: 20.2volt, S: 200mm/min and heat input 0.889 KJ/mm, ($\times 200$).

3.3. Effect of Weld Speed on Microhardness

Concerning the effect of welding speed on microhardness at welding current 170Amp and welding voltage 20.2V, the microhardness distribution in different zones; weld zone (FZ), heat affected zone (HAZ) and base metal (BZ) is shown in Fig. 10. The microhardness values of 166.6- 231 HV are observed at location within 1 mm from the base metal, through the HAZ across the weld metal. From the figure, it can be seen that the microhardness values increase with increasing welding speed. This is attributed to increase the cooling rate and decrease the grain size. This is in agreement with hardness results of Zhang and Roy [9]. Besides, the maximum microhardness of WM is 201, 212 and 231 HV with welding speed 100, 150.37 and 172.413 mm/min, respectively. Width of FZ and HAZ regions, were affected by heat input with various welding speeds. Table 5 shows the increase of width of FZ and the decrease of width of heat affected zone HAZ with the decrease of welding speed.

3.4 Effect of Weld Current on Microhardness

Concerning the effect of welding current on microhardness at welding speed 200 mm/min and welding voltage 20.2 volt, the microhardness distribution in different zones; weld zone (FZ),

heat affected zone (HAZ) and base metal (BZ) is shown in Fig. 11. The microhardness values of 166.6-247 HV are observed at location within 1 mm from the base metal, through the HAZ across the weld metal. These hardness results are partially in good agreement with literature. Güral, et al. [15], have found that maximum hardness values are measured in the area of weld metal (FZ). Nevertheless, in the present work, the maximum hardness is both in weld metal (FZ) and heat-affected zone (HAZ). The variation in properties across the weld can be attributed to several issues, essentially to residual stresses just created after welding.

Welding current is the most significant factor, which effected on the microhardness. The hardness decreases with increasing the welding current (heat input) which increases the width of WM and HAZ regions as shown in Fig. 11 and Table 5. This is due to the decrease of cooling rates when increasing welding current and this effect turns to decrease in the microhardness of the welded joint. This is as result of increasing of the grain size i.e. coarser grain in HAZ region. The microhardness reaches maximum value 203HV at the middle of weld metal FZ and drops gradually to the base metal 166.6HV.

3.5 Effect of Plate-Thickness on Microhardness

Plate thickness plays the essential role in the effects on microhardness. Fig. 12 shows the microhardness distribution in different zones; weld zone (FZ), heat affected zone (HAZ) and base metal (BM) at different welding current and welding voltage. The microhardness values of 167-253 HV in Fig. 12 are observed at location within 1mm from the base metal, through the HAZ across the weld metal. It is observed that the microhardness values decrease as plate thickness increases because of drop in the cooling rate and the increase in grain size of WM and HAZ. The peak microhardness value is 219, 212 and 208HV in HAZ region, respectively with increase of thickness. In addition, the width of HAZ is affected by plate thickness, where bigger HAZ width about 3.5mm was obtained at thickness (10mm), this is attributed to higher weld heat input; slower cooling rate [17], as compared with other plates. Width of FZ and HAZ regions, were observed Table 5, it shows an increase of width of FZ and heat-affected zone HAZ with the increase of plate thickness.

3.6. Effect of Heat Input on Impact Resistance

To evaluate the effect of heat input developed during the MIG welding at different parameters, on the impact strength, a set of three specimens is selected and the results of absorbed energy that obtained from the testing machine were tabulated in Table 6. In this table, it can see that an increase in heat input leads to drop in cooling rate [18] and it gives an effect of decreasing the impact strength within this value of current as shown in Fig. 13. From the experiments, it is shown that for the range of current 220-260Ampere, the impact strength of the weld and heat affected zone of the weld joint reduces. As a result, the higher heat input, the lower impact toughness value, this in agreement with literature [19].

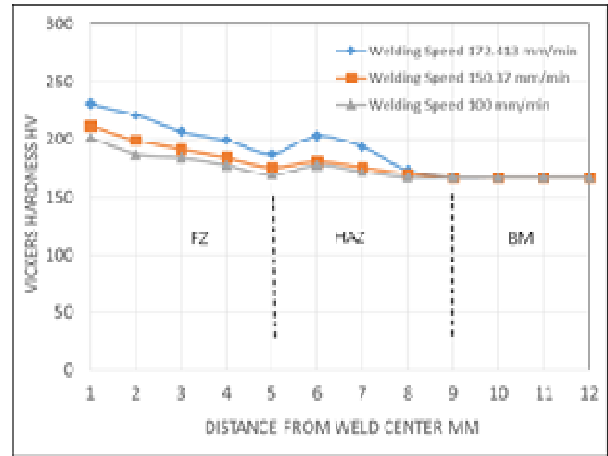


Fig. 10. Effect of Welding Speeds on Microhardness at welding current 170 Amp and welding voltage 20V.

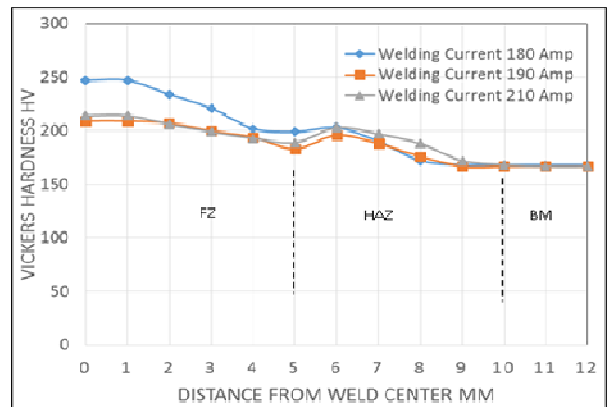


Fig. 11. Effect of Welding Current on Microhardness at Welding Speed 200mm/min and welding voltage 20.2volt.

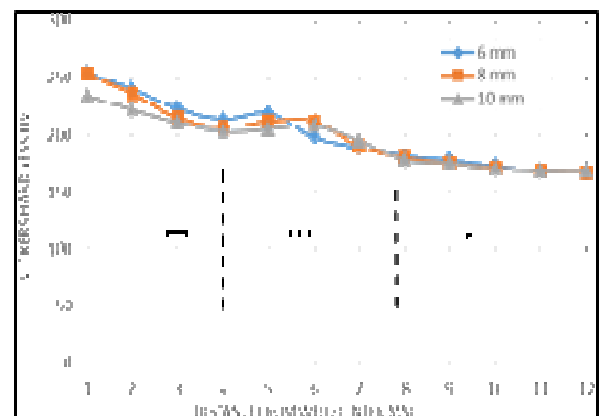


Fig. 12. Effect of Plate Thickness on Microhardness at different welding current and welding voltage.

Table 6,
Impact test results with plate thickness 10mm at welding currents (220, 240 and 260 Ampere).

Specimen Code.	Heat Input (KJ/mm)	Impact Energy (J)
A	1.2719	61.74
B	1.4546	54.4
C	1.6702	49.17

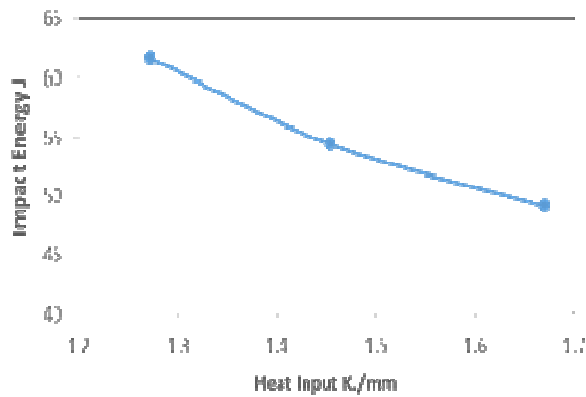


Fig. 13. The relationship between Impact energy and Heat Input at different welding parameters.

4. Conclusions

1. It is found that formation of phases; acicular ferrites (AF), Widmanstatten ferrites (WF) and polygonal ferrites (PF) in weld metal (WM) are affected by weld heat input.
2. Increasing welding current leads to increment in the heat input, this leads to a reduction in cooling rate, then increases the grain size of weld metal (WM) and heat affected zone (HAZ) and decreases the microhardness of the welded joint.
3. Increasing the welding speed, decreases the heat input (i.e. increases the cooling rate) which leads to increase the microhardness in WM and HAZ regions, decreases grain size in WM and HAZ regions..
4. Increasing plate thickness leads to increase the heat input and reducing the cooling rate, this leads to increase the grain size of WM and HAZ regions and decrease in the microhardness values.
5. Impact strength of the weld metal and heat affected zone HAZ of the weld joint reduces with increasing of heat input.

5. Notation

Q	Heat input (J/mm)
I	Welding Current (Ampere)
V	Welding Voltage (Volt)
S	Welding speed (mm/min)
n	Order of diffraction
d	Inter planer spacing distance (Å)
I _{corr}	Corrosion Current (μA/cm ²)
E _{corr}	Corrosion Potential (mV)
C.R	Corrosion rate (mm/year)
W	Equivalent weight (Grams)
R ²	Coefficient of determination
FZ	Fusion Zone
HAZ	Heat Affected Zone
WM	Weld Metal
BM	Base Metal
AF	Acicular Ferrite
WF	Widmanstatten Ferrite
PF	Polygonal Ferrite
MIG	Metal Inert Gas Welding
MMAW	Manual Metal Arc Welding
AWS	American Welding Society
MS	Martensite Start
MF	Martensite Finish
CF	Cold finishing
HF	Hot rolled

Greek letters

η	Welding efficiency (%)
λ	Wave length (Å)
θ	Diffraction angle (degree)
ρ	Density (g/cm ³)

5. References

- [1] The Procedure Handbook of Arc Welding, 14th Edition, The James F. Lincoln Arc Welding, 2000.
- [2] Gourd LM, Principles of Welding Technology, 3rd Edition. Edward Arnold, 1995.
- [3] J. Beddoes & M. J. Bibby, "Principles of Metal Manufacturing Processes", Carleton University, Canada, 1999.
- [4] J. Puchaicela, "Control of Distortion of Welded Steel Structures", Welding Journal, pp.49-52, 1998.
- [5] Kim IS, Sona JS, Kim IG, Kim JY and Kim OS., "A study on relationship between process variables and bead penetration for robotic CO₂ arc welding", J. Mater. Process. Technol. 136, pp. 139–145, 2003.

- [6] Han GuoMing, Yun ShaoHui, Cao XinHua, Li JunYue, "Acquisition and pattern recognition of spectrum information of welding metal transfer", *J. Mater. & Design*, 24, 699–703, 2003.
- [7] *Welding Handbook Volume 4, "Metals and their Weldability"*, American Welding Society (ASM), Seventh.
- [8] Richard S.Sabo, "The procedure Handbook of Arc welding ", the lincoln electric company, Cleveland, Ohio44117, Australia, 1999.
- [9] Zhang. W. and G.G.Roy, "Modeling of Heat Transfer and Fluid Flow During Gas Tungsten arc Spot Welding of Low Carbon Steel", *Journal of Applied Physics*, March , , Vol. 93, No. 5, 2003.
- [10] Ueji, R., Fujii, H., Cui, L., Nishiokioka, A., Kunishige, K. and Nogi, K., "Friction Stir Welding of Ultrafine Grained Plain Low-Carbon Steel Formed by the Martensite Process", *Materials Science and Engineering: A*, 423, 324- 330, 2006. <http://dx.doi.org/10.1016/j.msea.2006.02.038>
- [11] Easterling, K.E., "Modeling the Weld Thermal Cycle and Transformation Behavior in the Heat Affected Zone", In: Cerjak, H. and Easterling, K.E., Eds., *Mathematical Modeling of Weld Phenomenon*, The Institute of Materials, 1998.
- [12] Marashi, P., Pouranvari, M., Amirabdollahian, S. and Abedi, G., "Microstructure and Failure Behavior of Dissimilar Metal Spot Welds between Low Carbon Steel, Galvanized and Austenitic Stainless Steels. *Materials Science and Engineering: A*, 420, pp. 175-180, 2008. <http://dx.doi.org/10.1016/j.msea.2007.07.007>
- [13] G. R. Stewart, A. M. Elwazri, R. Varano, N. Pokuty-lowicz, S. Yue and J. J. Jonas, "Shear Punch Testing of Welded Pipeline Steel," *Materials Science and Engineering A*, Vol. 420, No. 1-2, , pp. 115-121, 2006.
- [14] S. Lars-Eric, "Control of Microstructures and Properties in Steel Arc Welds," *Library of Congress Catalog-ing-in-Published Data*, British, 1994.
- [15] A. Güral, B. Bostan and A. T. Özdemir, "Heat Treatment in Two Phase Region and its Effect on Welding of a Low Carbon Steel," *Materials and Design*, Vol.28, No. 3, pp. 897-903, 2007.
- [16] Gery, H., Long, P. and Maropoulos, E., "Effects of welding speed, energy input and heat source distribution on temperature variations in butt joint welding", *Journal of Material Processing Technology*, 167, pp 393-401, 2005. <http://dx.doi.org/10.1016/j.jmatprotec.2005.06.018>
- [17] David S.A, S.S.Babu, & J.M.Vitek, "Welding Solidification and Microstructure", *Oak Ridge National Laboratory*, Vol. 32, No. 3, 2003.
- [18] Odd M.Akselsen, Ragnhild and Vigdis Olden, "Effect of Phase Transformations on Residual Stresses in Welding of Stainless Steel", *International Journal of Offshore and Polar Engineering (ISSN 1053-5381)*, Vol. 17, No. 2, pp. 145–151, 2007.
- [19] Wan Shaiful Hasrizam Wan Muda, Nurul Syahida Mohd Nasir, Sarizam Mamat and Saifulnizan Jamian, "Effect of welding heat input on microstructure and mechanical properties at coarse grain heat affected zone of ABS grade a steel", *ARNP Journal of Engineering and Applied Sciences*, Vol. 10, No 20, pp. 9487- 9495, 2015.

دراسة تأثير الحرارة المتولدة اثناء اللحام على البنية المجهرية، الصلادة، والامتانة لفولاذ AISI 1015

احسان خلف رثيع***

عباس شياع علوان**

عماد خميس حمد*

*،***، كلية الهندسة/جامعة الانبار

** كلية الزراعة/جامعة بغداد

*البريد الالكتروني: emkh7676@gmail.com

**البريد الالكتروني: drabbasshalwan@gmail.com

***البريد الالكتروني: ih77san@yahoo.co.uk

الخلاصة

في الدراسة التجريبية هذه، تم استخدام اللحام الغازي المعدني الخامل للحام فولاذ منخفض الكربون (AISI 1015) باستخدام سلك لحام قطره (١,٥ ملم) نوعه (ER308L) والقطبية المطبقة قطبية مباشرة ذات تيار مباشر من قطب اللحام الى الوصلة، وتم لحام وصلة تناكبية على شكل الحرف (V) بتمريرة واحدة عند اسماك مختلفة (٦، ٨ و ١٠ ملم). تضمن الجانب العملي لهذه الدراسة، تحضير صفائح من الفولاذ الكربوني ذات ابعاد (٢٠٠ ملم x ١٠٠ ملم) وحواف ذات زاوية (٥٦°) من كلا جانبي وصلة اللحام، تم لحام وصلات اللحام المعدة عند متغيرات مختلفة وهي: تيار اللحام، سرعة اللحام والحرارة المتولدة وسمك وصلة اللحام. تم اجراء اللحام لثلاث مجاميع من العينات كل منها يضم ثلاث عينات. النتائج بينت ان الزيادة في الحرارة المتولدة اثناء اللحام تعمل على زيادة بنية فرايت فيدمنشتاتن والفرايت الابري وفرايت متعدد الجوانب في منطقة اللحام الانصهاري، ونقصان الحجم الحبيبي نتيجة معدل التبريد السريع (حرارة متولدة اقل). وايضا لوحظ زيادة الصلادة المايكروية مع نقصان الحرارة المتولدة اثناء اللحام، وزيادة في عرض منطقة اللحام والمنطقة المتأثرة بالحرارة مع زيادة الحرارة المتولدة اثناء اللحام. مقاومة الصدمة لوصلة الفولاذ الكربوني منخفض الكربون في منطقة اللحام تقل بزيادة الحرارة المتولدة اثناء اللحام، حيث ان اقل طاقة صدمة (٤٩,١٧ جول) نتجت عند اعلى حرارة متولدة (٢,٣٨٦ كيلوجول/ملم). لوحظ ايضا ان معدل التآكل لوصلة اللحام يزداد بزيادة تيار التآكل نتيجة الزيادة الحاصلة في تيار اللحام (زيادة الحرارة المتولدة)، بمعنى آخر فان مقاومة التآكل لوصلة اللحام تقل بزيادة كمية الحرارة المتولدة اثناء عملية اللحام.